Novel Stabilization Mechanism on Polar Surfaces: ZnO(0001)-Zn

Olga Dulub,[1] Ulrike Diebold,[1,*] and G. Kresse[2]

[1]*Department of Physics, Tulane University, New Orleans, Louisiana 70118*
[2]*Institut für Materialphysik and Centre for Computational Materials Science, Universität Wien, A-1090 Wien, Austria*
(Received 11 September 2002; published 8 January 2003)

The (1×1) terminated (0001)-Zn surface of wurtzite ZnO was investigated with scanning tunneling microscopy. The surface is characterized by the presence of nanosized islands with a size-dependent shape and triangular holes with single-height, O-terminated step edges. It is proposed that the resulting overall decrease of the surface Zn concentration stabilizes this polar surface. *Ab initio* calculations of test geometries predict triangularly shaped reconstructions over a wide range of oxygen and hydrogen chemical potentials. The formation of these reconstructions appears to be electrostatically driven.

The stability of polar surfaces is one of the puzzles of modern surface science [1]. Ionic crystals that consist of alternating layers of oppositely charged ions, stacked parallel to such surfaces, produce an accumulating normal dipole moment. Electrostatic considerations [1,2] show that this leads to an energetically highly unstable situation. Crystals with polar surfaces generally facet or exhibit massive surface reconstructions. In some cases, however, polar surfaces are quite stable, and the stabilization mechanisms are currently being debated [1]. The basal planes of ZnO are prime examples of stable polar oxide surfaces [3,4]. ZnO is widely used in catalysis, gas sensing, and in the fabrication of microelectronic devices. The geometric, electronic, and defect surface structures play a role in all of these applications; hence the definite identification of the stabilization mechanisms of polar ZnO surfaces and the resulting surface properties would be of high practical interest. Moreover, clarifying how the polarity is canceled on ZnO could help understand the stability of other polar surfaces.

ZnO crystallizes in the hexagonal wurtzite structure and can be described schematically as a number of alternating planes composed of fourfold-coordinated O^{2-} and Zn^{2+} ions, stacked along the c axis with alternating distances $R_1 = 0.69$ Å and $R_2 = 1.99$ Å, respectively. Cutting the crystal perpendicular to the c axis always creates a Zn-terminated (0001) surface on one side of the crystal and an O-terminated (000$\bar{1}$) surface on the other side. These two polar surfaces have different physical and chemical properties [5]. If the crystal is uncompensated, the net dipole moment diverges with increasing thickness and the electrostatic potential increases monotonically. Electrostatic considerations [6] as well as electronic structure calculations [1] show that a rearrangement of charge on both outermost layers of a ZnO crystal will cancel the polarity. If the Zn-terminated surface is less positive and the O-terminated surface layer less negative by a factor of $R_2/(R_1 + R_2) \sim 0.75$ [1,6], a counterfield is created that quenches the macroscopic dipole moment. This reduction in surface charge density can occur

through three principal mechanisms: (1) creation of surface states and transfer of negative charge from the O to the Zn face; (2) removal of surface atoms; and (3) positively (negatively) charged impurity atoms on the O (Zn) surfaces.

Thus far it is still unresolved which one of the three stabilization mechanisms is at work on ZnO. *Ab initio* calculations of (1×1) terminated surfaces favor mechanism (1) [1,3,7]. However, the expected 2D metallic surface states [3,7] have not been observed in photoemission experiments [8,9]. The calculations predict inward relaxations for the outermost O (Zn) ions on both polar surfaces [3,7], in reasonable agreement with experimental results on the ZnO(000$\bar{1}$)-O surface. However, a slight outward relaxation of the outermost Zn layer on (0001)-Zn is found experimentally [10,11]. Surface x-ray diffraction results on the ZnO(0001)-Zn surface could best be fitted by allowing a 0.75 occupancy of the topmost surface layer [11], in agreement with stabilization mechanism (2). How this nonstoichiometry is achieved is not known, a random removal of 1/4 Zn atoms was used in Ref. [11]. Interestingly, the simplest and most-ordered configuration of missing Zn atoms, i.e., a (2×2) configuration of point defects, has never been observed [8,11,12]. Recent calculations suggest that the adsorption of H (OH) on the O (Zn) side is energetically unfavourable, but only a very high coverage was considered [3].

Scanning tunneling microscopy (STM) results presented in this paper provide the first direct evidence for stabilization mechanism (2) on the Zn-terminated surface. The removal of surface Zn atoms occurs through the formation of a high density of one-layer-high, O-terminated step edges and results in the formation of "magic" islands with a size-dependent shape that is correlated to the stabilizing surface stochiometry. *Ab initio* density functional theory calculations of test structures confirm the stability of a surface morphology with triangularly shaped one-layer-deep holes over a wide range of oxygen and hydrogen chemical potentials. Under suitable conditions (abundance of H and O), a large amount of

hydroxyl groups can adsorb on the surface, indicating a competition between mechanisms (2) and (3).

All experiments were performed in UHV at a base pressure of 1×10^{-10} mbar. Five hydrothermally grown samples from different vendors with a polished (0001)-Zn face were used. The samples exhibited colors ranging from clear to light yellow. Details of sample preparation are described in a complementary study on other low-index ZnO faces; see Ref. [13]. Prior to mounting the crystals on the holder, the Zn and O sides were identified by their chemical etching behavior (the oxygen face of ZnO etches in HCl solution more rapidly than the zinc face). The correct sample orientation was confirmed by low-energy He$^+$ ion scattering (LEIS) performed *in situ*. Results presented here were obtained on samples after sputtering with 1 keV Ar$^+$ for 15 min and annealing at 700 °C for 5 min in UHV. Annealing at lower temperatures (500 °C–700 °C) gives the same surface morphology; annealing at higher temperatures causes a macroscopic roughening of the surface. Sample cleanliness was confirmed by LEIS and x-ray photoelectron spectroscopy. Of particular interest for the stabilization mechanism of the Zn-terminated surface is the presence of adsorbed hydrogen. Becker *et al.* reported that atomic H, or exceptionally large doses of molecular H$_2$, will form a (1×1) overlayer [12]. Such conditions were avoided in the present experiments. The surface yielded a sharp (1×1) low-energy electron diffraction pattern with a sixfold symmetry. STM images were recorded in the constant-current topographic mode at sample biases of $+1.7$ to $+2.2$ V and tunneling currents of 0.4 to 1.4 nA.

The (0001)-Zn surface shows the characteristic topography pictured in Fig. 1(a). All terraces are separated by step heights of ~2.7 Å; this value corresponds to the distance between two neighboring Zn layers (half a unit cell) in the ZnO structure. The surface exhibits a high density of one-layer-deep triangular pits. The inset of Fig. 1(a) shows that the smaller pits have a round shape, which might be partially caused by an STM tip broadening effect. The average distance between such smaller pits is ~8 Å. The line profile of a typical pit shows that it is also one layer deep [the somewhat smaller value measured in the line profile in Fig. 1(a) (~ 2.4 Å) is caused by the finite size of the STM tip]. The largest pits have triangular holes inside; see, for example, the two labeled "P" in Fig. 1(a). In addition to the pits, numerous islands of different sizes are observed on the terraces. These are also one layer high. Similar to the pits, all added islands have the shape of an equilateral triangle. Larger islands have multiple pits inside them. Interestingly, smaller islands (with side lengths ranging from 16 to 34 Å) have special shapes. The orientation and shape of their inner hole depends on the size of an island [Fig. 1(a), (i)–(iii)].

The presence of small islands and pits leads to an unusally high concentration of step-edge sites. All triangles on one terrace point in the same direction, indicating a termination with one type of atom only. On

the ZnO(0001)-Zn surface, oxygen step-edge atoms are threefold coordinated and zinc step-edge atoms are twofold coordinated. Hence it is expected (and confirmed by the calculations reported below) that the triangular terraces and pits on the surface exhibit exclusively O-terminated step edges. Such a step-edge termination is in line with compensation mechanism (2), as this increases the O concentration on each terrace.

If surface atoms carry the same charge as bulk atoms, mechanism (2) dictates a surface Zn/O ratio of 3/4 [1,6]. The models in Fig. 1 for the observed special small islands (i–iii) have been constructed with this value in mind. The number of O ions in an equilateral triangular
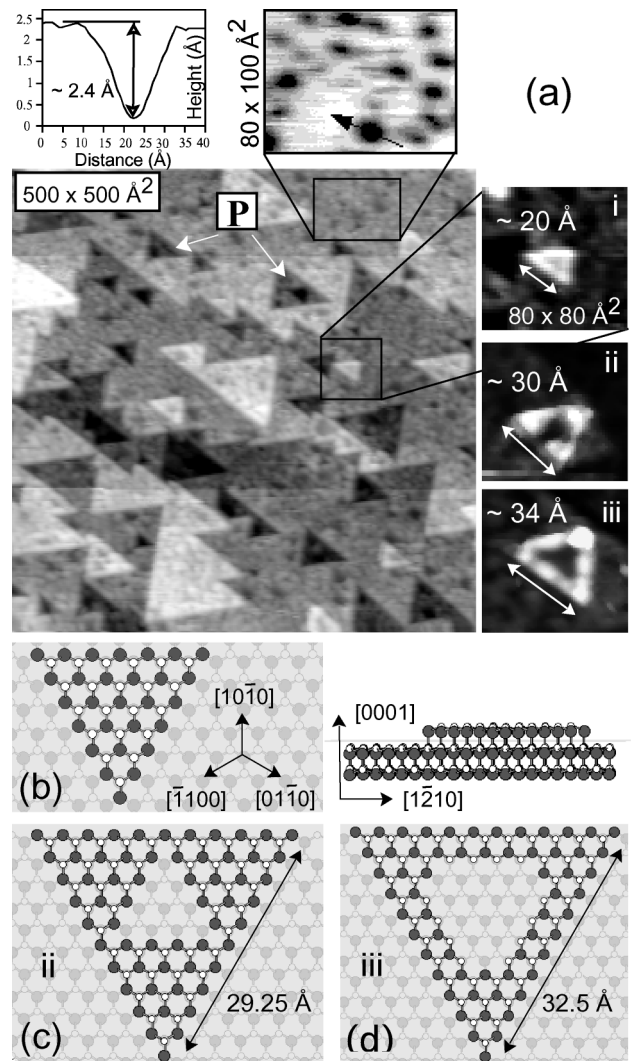

FIG. 1.   (a) Empty-states STM images of the (0001)-Zn surface. Terraces are covered by triangular islands and holes that are separated by single layer height steps. A high concentration of small holes is present on the terraces; see inset. The small images (i)–(iii) show small islands with special shapes that are characteristic for each island's size. (b) Top and side views of atomic model for the smallest observed island on the ZnO(0001)-Zn surface. (c),(d) Top view of models for islands (ii),(iii). Small white balls: Zn; large dark balls: O.

island is $n(n + 1)/2$, where n is the number of the edge O ions (on one side of the triangle). The number of Zn ions is $n(n - 1)/2$. For $n = 7$ the Zn to O ratio in the terrace is exactly the desired $3/4$; see the island in Fig. 1(b). Indeed, the smallest island size observed in STM images has this size (Zn edge–Zn edge distance ~ 16 Å). For the next bigger island with $n = 8$, an additional Zn atom has to be removed to keep the Zn to O ratio at the stabilizing value, this would explain the depression at the center of island (i) in Fig. 1(a). Following this scheme, an island with a side length of $n = 11$ is constructed [Fig. 1(c)]. It shows a perfect correspondence to the observed shape of an island of this size [image (ii) in Fig. 1(a)]. The most symmetric model for an $n = 12$ island [labeled (iii) in Fig. 1(a)] has the inner hole terminated by Zn atoms and is the largest island with a single hole observed. The model of this island is presented in Fig. 1(d). The number of configurations that provides excess O at step edges increases with the size of the island, and bigger islands in Fig. 1(a) have multiple holes.

While this analysis suggests that the observed surface morphology is related mainly to stabilization mechanism (2), it focuses on isolated islands rather than the whole surface. Many more small holes than magic islands are present, but tip broadening effects [see the line profile in Fig. 1(a)] make it difficult to determine their exact shape and to quantify the excess concentration of step-edge oxygen. In order to examine our hypothesis, we resort to *ab initio* calculations of test structures.

The calculations were performed with the Vienna *ab initio* simulation package (VASP) [14], using the projector augmented-wave method in the implementation of Ref. [15]. An energy cutoff of 280 eV and generalized gradient corrections were applied [16]. With this setting the lattice parameters of ZnO are found to be $a = 3.282$ Å, $c = 5.309$ Å, and $u = 0.378$, in good agreement with experiment. The surface was modeled by slabs with six double ZnO layers, where only the three topmost layers were allowed to relax, and the three bottom layers were kept frozen at the positions determined for the ideal oxygen terminated $(000\bar{1})$ surface.

Roughly 100 defect configurations were considered covering (4×4), (6×6), $(\sqrt{37} \times \sqrt{37})$, and $(\sqrt{48} \times \sqrt{48})$ supercells. To sample the band structure, k-points corresponding to a mesh of approximately 12×12 points in the primitive surface cell were chosen (relaxation was usually performed with the Γ point only). The investigated defect configurations included Zn vacancies, O adatoms at H3 (threefold hollow) and T4 (fourfold) sites (see Fig. 2), hydroxyl ad-groups at the H3 and T4 sites, H adsorption in various sites, and triangularly shaped pits with an edge length n between $n = 2$ and $n = 7$. These indentations were created by removing $n(n + 1)/2$ Zn atoms and $n(n - 1)/2$ O atoms. The phase diagram for equilibrium between the surface and independent H and O particle reservoirs is shown in Fig. 2. Clearly the stable surface depends on the surrounding gas phase [17]. The
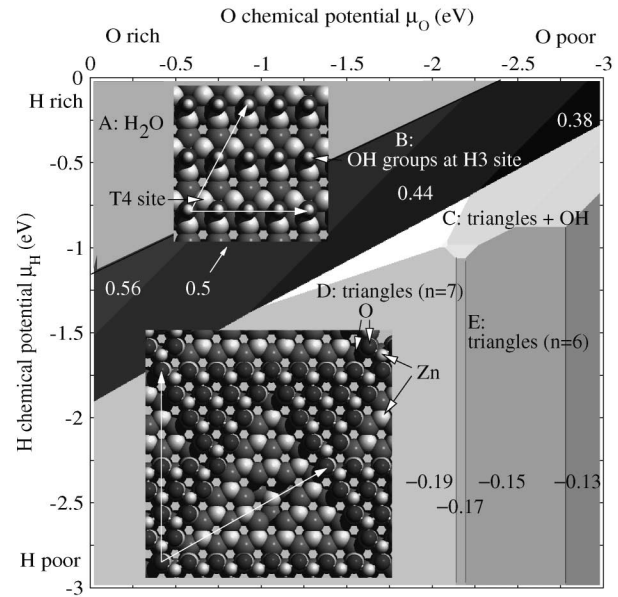

FIG. 2. Phase diagram of ZnO(0001)-Zn surface in equilibrium with H and O particle reservoirs controlling the chemical potentials, μ_H and μ_O. The chemical potentials can be related to the oxygen and hydrogen partial pressure p_x through $\mu_x(T, p_x) = \mu_x(T, p_x^0) + 1/2 k_B T \ln(p_x/p_x^0)$ [17]. Preparation conditions of 800 K and 10^{-10} mbar correspond to $\mu_O < -1.9$ eV and $\mu_H < -1.4$ eV. The upper left area (A) indicates the conditions under which H$_2$O condensates on the surface. The dark and bright areas correspond to an OH covered surface (B) and triangular reconstructions (D + E), respectively. The area C in between corresponds to conditions in which hydroxyl groups adsorb on the terraces and in the triangular pits ($\theta_{OH} < 0.06$ ML). Positive numbers indicate the OH coverage θ_{OH} and negative numbers indicate the effective Zn deficiency θ_{Zn} per surface area. The two insets show optimized structures corresponding to the area. The basis vectors of the supercells are indicated by arrows.

calculations indicate that, under H rich conditions, hydroxyl groups adsorb at the H3 site (area B in Fig. 2). A significant repulsion between them is observed leading to a gradual increase of the OH coverage with increasing hydrogen or oxygen concentration. Competing processes, such as adsorption of atomic H on the Zn-terminated surface, are thermodynamically less stable, which does not preclude that such structures can form under suitable kinetic conditions [12].

At hydrogen poor conditions, relevant for the present experimental study, only triangularly shaped reconstructions are stable on the surface (areas D and E in Fig. 2). The adsorption of oxygen at the H3 site or Zn vacancies are typically 0.3 eV per defect atom less favorable than triangles. The size of the triangles and the effective Zn vacancy concentration θ_{Zn} varies with the oxygen concentration: oxygen poor conditions favor Zn rich terminations. But under relevant conditions, the Zn deficiency θ_{Zn} remains in a fairly narrow window, between -0.19 and -0.125 monolayer (ML). A Zn/O ratio of $3/4$ is not reached, indicating that mechanism (1) is operative at

least to some extent. The limited number of models considered allows only tentative statements about the size and shape of the triangles. At oxygen poor conditions, a triangular pit with an edge length $n = 6$ in the $(\sqrt{48} \times \sqrt{48})$ supercell is most stable (area E, $\theta_{Zn} = -6/48 \approx -0.13$). With increasing oxygen chemical potential, the Zn deficiency gradually increases. This is accomplished by the creation of an additional Zn vacancy in the center of the pit (area E, $\theta_{Zn} = -0.15$), and then by an increase of the edge length to $n = 7$ with a Zn vacancy in the center (area D, $\theta_{Zn} = -0.17$). Finally, an additional triangular indentation with $n = 2$ forms in the center of the first pit (area D, $\theta_{Zn} = -0.19$). Hence the calculations agree with the experiment in favoring triangular reconstructions with additional features in larger triangles.

To determine why triangles are more stable than Zn vacancies, first note that the number of cleaved Zn-O bonds is exactly identical for n isolated Zn vacancies and a triangular pit with an edge length n. In a second moment approximation (taking into account nearest neighbor interactions only), an identical stability for both models is hence expected. The second finding is that relaxation increases the stability of triangles compared to Zn vacancies only by roughly 30%. Therefore, release of surface stress plays a role but it is not the dominant factor. The main reason for the stability of triangles is revealed by a simple electrostatic Madelung model. In this model, the assigned ionic charge is $+2$ and -2 for the bulk Zn and O atoms and $+1.5$ (-1.5) for the terminating Zn (O) atoms of the defect free (0001) [(000$\bar{1}$)] surface. The reduced ionicity at the surface is compatible with the charge transfer picture discussed in Refs. [1,3], and leads to a convergent Madelung energy for the polar surface. To model the defective surfaces, the ionicity for the outermost Zn atoms is set to $1.5/(1 + \theta_{Zn})$, which ensures that the Madelung energy remains well defined. The important point is that this simple electrostatic model predicts the energy differences between unrelaxed defect configurations to within 20%, if a dielectric constant of 5 is assumed. The Madelung energy hence favors triangles over isolated vacancies in quantitative agreement with the *ab initio* calculations, which is a strong indication that electrostatics are responsible for the stabilization of triangles. The likely explanation for this behavior is that the three oxygen atoms left back upon creation of a Zn vacancy experience a strong mutual repulsion, which is relieved by the reconstruction.

The experimental and theoretical results suggest that the observed "rugged" topography of the ZnO(0001)-Zn surface is due to electrostatics. Even "pristine" ZnO surfaces will exhibit a high concentration of step edges. This has obvious consequences for surface properties. For example, Zn-terminated polar faces are reactive for cata-lytic dehydrogenation and oxidation reactions. It has been suggested [5] that these occur at pairs of acid/base sites. An abundance of such paired sites would be provided by the threefold coordinated Zn atoms next to step-edge oxygens [13]. The special morphology of the ZnO(0001)-Zn surface also has ramifications for the growth of perfect ZnO epilayers needed for novel ZnO-based electro-optical devices [18]. Step edges act as important nucleation sites, and their presence can dramatically influence the observed growth behavior. In addition to pointing toward a novel mechanism for relieving the dipole moment on polar surfaces, these results are possibly of relevance for emerging applications of this exciting material.

*Electronic address: diebold@tulane.edu
[1] C. Noguera, J. Phys. Condens. Matter **12**, R367 (2000).
[2] P. W. Tasker, J. Phys. C **12**, 4977 (1979).
[3] A. Wander and N. M. Harrison, J. Chem. Phys. **115**, 2312 (2001).
[4] A. Wander, F. Schedin, P. Steadman, A. Norris, R. McGrath, T. S. Turner, G. Thornton, and N. M. Harrison, Phys. Rev. Lett. **86**, 3811 (2001).
[5] J. M. Vohs and M. A. Barteau, Surf. Sci. **176**, 91 (1986).
[6] R. W. Nosker, P. Mark, and J. D. Levine, Surf. Sci. **19**, 291 (1970).
[7] J. M. Carlsson, Comput. Mater. Sci. **22**, 24 (2001).
[8] W. Göepel, J. Pollmann, I. Ivanov, and B. Reihl, Phys. Rev. B **26**, 3144 (1982).
[9] R. T. Girard, O. Tjernberg, G. Chiaia, S. Soederholm, U. O. Karlsson, C. Wigren, H. Nylen, and I. Lindau, Surf. Sci. **373**, 409 (1997).
[10] H. Maki, N. Ichinose, N. Ohashi, H. Haneda, and J. Tanaka, Surf. Sci. **457**, 377 (2000).
[11] N. Jedrecy, M. Sauvage-Simkin, and R. Pinchaux, Appl. Surf. Sci. **162–163**, 69 (2000).
[12] T. Becker, S. Hovel, M. Kunat, C. Boas, U. Burghaus, and C. Wöll, Surf. Sci. **486**, L502 (2001).
[13] O. Dulub, L. A. Boatner, and U. Diebold, Surf. Sci. (to be published).
[14] G. Kresse and J. Furthmüller, Phys. Rev. B **54**, 11 169 (1996).
[15] G. Kresse and D. Joubert, Phys. Rev. B **59**, 1758 (1999).
[16] J. P. Perdew, J. A. Chevary, S. H. Vosko, K. A. Jackson, M. R. Pederson, D. J. Singh, and C. Fiolhais, Phys. Rev. B **46**, 6671 (1992).
[17] K. Reuter and M. Scheffler, Phys. Rev. B **65**, 035406 (2002).
[18] M. Zamfirescu, A. Kavokin, B. Gil, G. Malpuech, and M. Kaliteevski, Phys. Rev. B **65**, 161205 (2002).